POSSIBLE ROLE OF HELIX–COIL TRANSITIONS IN THE MICROSCOPIC MECHANISM OF MUSCLE CONTRACTION

JEFFREY SKOLNICK

Department of Chemistry, Institute of Macromolecular Chemistry, Washington University, St. Louis, Missouri 63130

ABSTRACT   Local helix–coil transitions in the coiled coil portion of myosin have long been implicated as a possible origin of tension generation in muscle. From a statistical mechanical theory of conformational transitions in coiled coils, the free energy required to form a randomly coiled bubble in the hinge region of myosin of the type conjectured by Harrington (Harrington, W. F., 1979, *Proc. Natl. Acad. Sci. USA*, 76:5066–5070) is estimated to be ~25 kcal/mol. Unfortunately this is far more than the free energy available from ATP hydrolysis if the crossbridges operate independently. Thus, in solution such bubbles are predicted to be absent, and the theory requires that the rod portion of myosin be a hingeless, continuously deforming rod. While such bubble formation in vivo cannot be entirely ruled out, it appears to be unlikely. We further conjecture that in solution the swivel located between myosin subfragments 1 and 2 (S-2 and S-1) is due to a locally random conformation of the chains caused by the presence of a proline residue at the point that physically separates the coiled coil from the globular portion of myosin. On attachment of S-1 to actin in the strong binding state, the configurational entropy of the random coil in the swivel region is greatly reduced relative to the case where the ends are free. This produces a spontaneous coil-to-helix transition in the swivel region that causes rotation of S-1 and the translation of actin. Thus, the model predicts that the actin filaments are pushed rather than pulled past the thick filaments by the crossbridges. The specific mechanism of force generation is examined in detail, and a simple statistical mechanical realization of the model is proposed. We find that the model gives a substantial number of qualitative and at times quantitative predictions in accord with experiment, and is particularly appealing in that it provides a simple means of free energy transduction—the well known fact that topological constraints shift the equilibrium between helical and random coil states.

INTRODUCTION

Although the widely accepted crossbridge theory of muscle contraction is now over thirty years old (Huxley, 1957, 1969, 1971), elucidation of the microscopic mechanism of force generation has remained elusive. As recently summarized in the reviews of Highsmith and Cooke (1983) and Harvey and Cheung (1983), there have been to date basically six classes of models proposed for the force-generating step: (*1*) Somehow a global conformation change of the acto–S1 complex occurs that causes rigid myosin subfragment 1 (S-1) to rotate with respect to actin, which remains rigidly fixed (Huxley, 1969; Huxley and Simmons, 1971). (*2*) S-1 is rigidly bound to actin; within S-1, a global conformational change occurs (Huxley, 1969; Goody and Holmes, 1983; Highsmith and Eden, 1986). (*3*) S-1 and actin are firmly bound together; the rolling action of actin produces the requisite rotation of S-1 and translation of the thin filament (Huxley, 1974). (*4*) There is a helix-to-random coil transition within myosin subfragment 2 (S-2), perhaps coupled with a counter rotation of S-1 in the direction opposite to the motion of the thin filaments (Harrington, 1971, 1979). (*5*) There is an elastic region within S-2 whose contraction provides the power stroke

(Huxley and Simmons, 1971). (*6*) S-1 and actin never come into physical contact; a change in the electrostatic charge of S-1 produces the requisite force on actin (Iwazumi, 1979).

As much experimental evidence exists that appears to make models *3* and *6* untenable (Highsmith and Cooke, 1983), we shall not discuss them further.

Since the rod portion of myosin is a coiled coil and since a number of theoretical advances have been made towards understanding the character of the helix–coil transition in such systems (Skolnick, 1983, 1984, 1985a,b, 1986; Skolnick and Holtzer, 1982a,b, 1985, 1986; Chen and Skolnick, 1986), we use a statistical mechanical theory to examine the role of such conformational transitions in the microscopic mechanism of muscle contraction. We begin by exploring the plausibility of model *4* and conclude that the free energy requirements make such a mechanism of muscle contraction unlikely, because loop entropy excludes the randomly coiled bubbles between interacting helices whose existence is central to model *4*. However, the very same physical effect would lead, when S-1 is strongly bound to actin, to a spontaneous coil-to-helix transition in the portion of S-2 attached to S-1, if such a region was in the random coil state before binding. We argue below that

this local conformational transition could produce the torque on S-1 required for the rotation of S-1 and concomitant translation of the thin filaments that is implicitly, if not explicitly, conjectured to occur in models _1_ and _2_. A simple mathematical realization of the model is developed and qualitative predictions of the theory are discussed. In what follows, all assumptions crucial to the theory will be numbered and italicized, whereas those assumptions merely used for the computational realization will appear in italics.

FREE ENERGY REQUIREMENTS OF THE HELIX–COIL TRANSITION IN THE HINGE REGION OF MYOSIN

The possible existence of a "hinge" or "melted" interior portion of myosin rod (e.g., Highsmith et al., 1977) has been invoked in several models of muscle contraction. To rationalize the apparently constant force generated per crossbridge at variable filament separation (Page and Huxley, 1963; Gordon et al, 1966), H. E. Huxley (1969) proposed the existence of a "hinge" region at the LMM–heavy meromyosin (HMM) junction of myosin rod to allow the S-1 heads to swing out and come in contact with the thin filament. Presumably the hinge would arise from local denaturation in a portion of S-2, although in the original proposal the conformation of the coiled coil in the hinge region is left unspecified. Actually, the essentials of the mechanism could be also achieved if S-2 was simply a continuously deforming rod. We return to this point below.

The possibility that a helix–coil transition could conceivably provide the requisite tensile force necessary for muscle contraction has been recognized for a long time (Hill, 1952, 1953; Flory, 1956_a,b_). However, the microscopic model has been fully developed by Harrington (1971, 1979) and Tsong et al. (1979). In outline, the conjectured sequence of events is: Subsequent to the strong binding of S-1 to actin, S-2 swings away from the thick filament, and a part of the structure, designated by Harrington (1979) as the force-generating element is destabilized and undergoes a helix-to-random coil transition, thus forming a constrained random coil bubble between pairs of interacting α-helices (see Fig. 1). The force-generating element is conjectured to consist of 201 residues per chain and originates at the LMM–HMM junction. For a chain composed of n residues, the root-mean-square end-to-end distance, $\langle R^2 \rangle^{1/2}$, in a helical rod is proportional to n, whereas in a random coil it is proportional to $n^{1/2}$. If S-2 undergoes a helix-to-coil transition, there will be an entropic force in the direction of contraction of the end-to-end distance. It is conjectured that this entropic force produces muscle contraction.

Support for such a "hinge" or random coil bubble in myosin rod in solution comes from electric birefringence measurements (Bernengo and Cardinaud, 1982; Cardi-
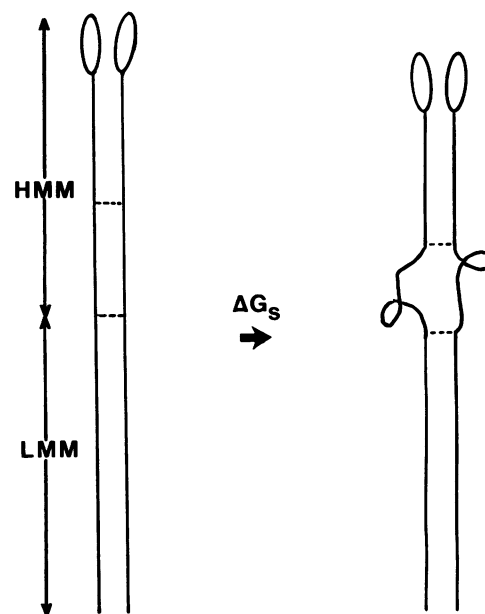

FIGURE 1 Schematic representation of the helix-to-random coil transition conjectured to occur in the Harrington (1971, 1979) mechanism of muscle contraction. Helical conformations are represented by straight lines and random coil conformations are depicted by wavy lines. The force-generating element is located between the pair of dotted lines.

naud and Bernengo, 1985), although more recent birefringence and light scattering studies (Hvidt et al., 1984), as well as viscoelastic measurements (Rosser et al., 1978; Hvidt et al., 1982, 1984) and fluorescence depolarization studies (Harvey and Cheung, 1983) show no evidence for a hinge. Rather, myosin appears to be a slightly flexible rod whose persistence length is 1,300 Å at high ionic strength (Hvidt et al., 1982, 1983). Moreover, the susceptibility of the LMM–HMM junction to enzymatic attack has been interpreted to indicate the presence of a random coil region (Sutoh et al., 1978). However, as chemical lability and chain flexibility are not necessarily identical (Harvey and Cheung, 1983), these results could be equally well rationalized by an enhanced chemical reactivity due to a particular local constellation of amino acids. Finally, electron microscopy studies show evidence of a bend in the myosin rod; however, the exact location depends on the technique used (Elliot and Offer, 1978; Takahashi, 1978).

A recently developed statistical mechanical theory of the helix–coil transition in two-chain, coiled coils (Skolnick, 1983, 1984, 1985_a,b_, 1986; Skolnick and Holtzer, 1986) allows us to estimate the free energy required to form a random coil bubble of the type conjectured in model _4_ for myosin rod in solution; the detailed calculation may be found in Appendix A (see Eqs. A1 and A2 and attendant discussion). We should point out that an important feature of the theory is that, in a coiled coil, residues participating in a randomly coiled bubble between pairs of interacting helices (Fig. 1) are highly constrained. It is essential that

the two ends of the random coils in each chain touch in order that the two pairs of α-helices be side-by-side and interacting. Thus, relative to the case where the ends are free, the random coil states experience a severe reduction in their configurational entropy. This effect is known as loop entropy (Schellman, 1955; Flory, 1956b; Jacobson and Stockmayer, 1950) and its occurrence in polymers (Jacobson and Stockmayer, 1950) and in DNA (Poland and Scheraga, 1969) is well documented and has been invoked, for example, to rationalize the enhanced thermal stability of RNase A on introduction of an extrinsic crosslink (Lin et al., 1984). Similarly it plays an important role in coiled coils.

The analysis in Appendix A indicates that a conservative value for the free energy change in vivo at 37°C for the process depicted in Fig. 1 is $+25.3$ kcal/mol, to which loop entropy contributes $\sim +6.2$ kcal/mol. In the above, we assume that the constrained random coil bubble contains 146 residues per chain, having corrected a minor error of Harrington in estimating the relevant mean-square end-to-end distance.

The free energy of ATP hydrolysis under the physiological conditions surrounding the myofilament is ~ 14 kcal/mol at 37°C (Hill, 1977). Furthermore, it is known that the thermodynamic efficiency of muscle in converting ATP hydrolysis into work is $\sim 50\%$ (Wilkie, 1975; Woledge et al., 1985). If we assume that one ATP is split per crossbridge cycle and each crossbridge in myosin acts independently, there is an apparent free energy deficit of ~ 11 kcal/mol, even assuming 100% efficiency of free energy transduction. If we take the experimentally observed efficiency of 50%, the deficit further increases to ~ 18 kcal/mol and the free energy of ATP hydrolysis essentially just balances the destabilization of bubbles due to loop entropy alone. The second possibility, of course, is that both crossbridges hydrolyze ATP simultaneously. Then, since the helix–coil transition must simultaneously occur in both chains of the myosin coiled coil for $\langle R^2 \rangle$ to decrease, if both heads are attached to actin, they must work in unison. However, this requires that the efficiency of free energy transduction be close to $\sim 90\%$, in our opinion, an unrealistically high value. Moreover, the assumption that both heads must work together to generate tension is invalidated by the results of Cooke and Franks (1978) who found that single-headed myosin will also generate tension. Even given single-head attachment, there is also the question of how ATP hydrolysis at the active site of S-1 influences a helix–coil transition hundreds of angstroms away (Highsmith and Cooke, 1983), although an interesting mechanism has been proposed by Harrington (1971). Thus, while it is not impossible that some other mechanisms exists for providing the additional free energy required to denature S-2 in the hinge region, none is known at present. Moreover, because of the temperature dependence of the free energy of the

helical states, the free energy deficit will increase as the temperature decreases, even though muscles are known to work over a wide temperature range (Ford et al., 1977). Thus, while the above analysis cannot prove that model 4 is invalid, it suggests it to be rather unlikely.

This crude analysis further suggests that because of the huge loop entropic price paid to form constrained randomly coiled bubbles, a hinge resulting from these conformational states does not occur in myosin rod in solution. While the results quoted above confined bubble formation to a specific region, statistical mechanics permits bubbles to occur in principle at any location within the myosin rod. However, when we applied the theory of the helix–coil transition of two-chain, coiled coils (Skolnick, 1984, 1985 a, b) to a homopolymeric analogue of myosin rod we find that, over the entire course of the helix–coil transition, >99.99% of the molecules are predicted to be devoid of randomly coiled bubbles between interacting helices. Basically, because of loop entropy, there is a single interacting pair of helices per molecule; of course that coiled coil segment may be of arbitrary length and may occur in any location. The interacting helical stretch may be preceded and/or followed by regions of alternating random coils and non-interacting α-helices, a representative conformation of which is shown in Fig. 2. Thus, the statistical mechanical theory demands that the coiled coil portion of myosin
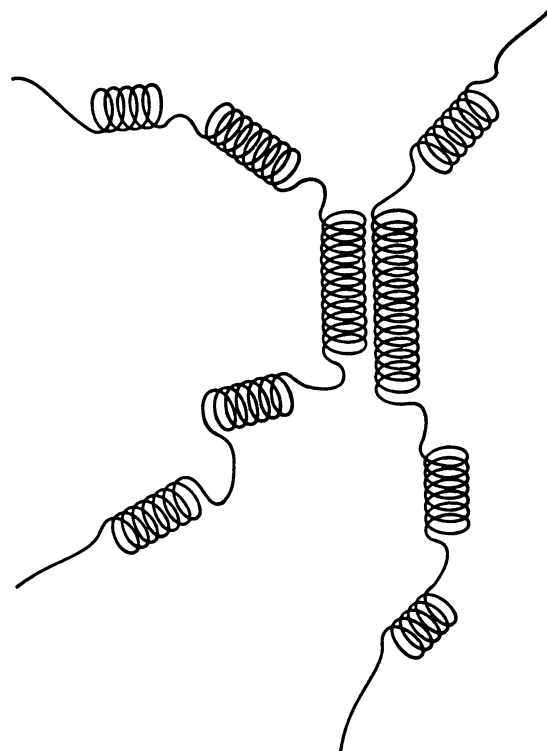

FIGURE 2 Schematic conformation of myosin rod in solution at an intermediate value of the average helix content based on the statistical mechanical theory of the helix–coil transition in coiled coils (Skolnick, 1984).

behaves like a continuously deforming, rather than once-broken, rod.

PROPOSED MECHANISM OF MUSCLE CONTRACTION

We begin by describing below the necessary assumptions of the coil-to-helix transition model of the power stroke, along with a discussion detailing the justification for these assumptions.

ROLE OF LIGHT MEROMYOSIN (LMM) AND THE ROD PORTION OF S-2

The present analysis suggests that hinges formed from random coil bubbles do not occur. This, however, only slightly modifies H. E. Huxley's (1969) original proposal: *(I) In a muscle, we envision LMM as always remaining attached to the thick filaments, consistent with the fact that it is insoluble in aqueous solution, and envision long S-2, which is soluble in aqueous solution, as a continuously deforming rod that allows the crossbridge to attach to actin.* As mentioned above, this result is based on dynamic viscosity measurements (Rosser et al., 1978; Hvidt el al., 1982); the persistence length of myosin rod is 1,300 Å (Hvidt et al., 1982, 1983). Hence, in solution, as originally pointed out by Hvidt et al. (1982), the NH_2-termini of S-2 could easily lie at least 260 Å away from the thick filament, more than enough to span the distance between the thin and thick filaments at all sarcomere lengths (Morawetz, 1965). So far then, Huxley's hinge between LMM and S-2 merely has been replaced by a slightly flexible, uniformly deforming rod. However, this is not to indicate that all of S-2 is passive during the course of muscle contraction. We next take up this point.

ROLE OF THE SWIVEL

There is considerable experimental evidence that, in solution at least, a very flexible swivel exists at the joint between S-1 and myosin rod (Mendelson, 1973; Thomas, 1978; Kobayashi and Totsuka, 1975; Harvey and Cheung, 1983). *(II) We conjecture that in an unconstrained myosin molecule, the conformational state giving rise to the swivel is a local random coil region located near the S-1–S-2 interface.* The existence of such a region is consistent with NMR studies, which indicate that the highly mobile component involving a portion of S-1 has spectra similar to that of a denatured protein (Highsmith et al., 1979; Eads and Mandelkern, 1984). Perhaps a portion of the spectra may be due to the conjectured random coil conformation giving rise to a swivel. Moreover, there is evidence that a proline is present at the S-1–S-2 junction (Karn et al., 1983). Since even a single proline acts as a "stop" to α-helix propagation, the α-helical, coiled coil region of of myosin would be terminated, and such a residue would act to physically separate the coiled coil region from the globular portion of myosin.

From the point of view of the α-helix, the proline is equivalent to introducing a free end, and it is well known from helix–coiled theory that free ends result in the fraying of α-helices (Poland and Scheraga, 1979). In other words, they favor random coil formation. Thus, within the swivel, there is a putative random coil region, a portion of which is assumed to be structurally part of S-2. The conformation of the swivel on the S-1 side containing the proline may or may not be partially randomly coiled. In the discussion below, the swivel region adjacent to the globular portion of S-1 is assumed to possess sufficient flexibility to allow S-1 to rotate (actually the latter assumption is not even required; the theory developed below predicts that the S-2 portion of the swivel is always partially randomly coiled). A schematic representation of myosin in solution, including a schematic blow up of the swivel region, is shown in Fig. 3. *(III) Moreover, since each chain contains a random*
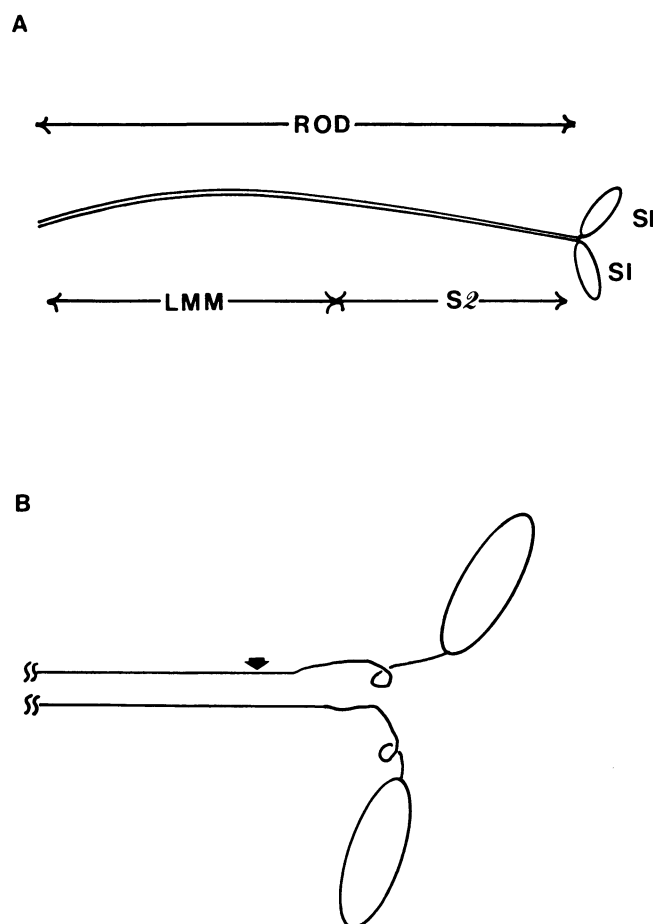
A

B

FIGURE 3 (*A*) Schematic representation of a typical conformation of myosin in solution indicating the location of the LMM, S-2, and S-1 portions of the molecule. (*B*) Blow up of a schematic conformation of the swivel region between S-2 and S-1 in solution showing the putative random coil conformation of the swivel. In each of the two chains the force-generating region lies to the right of the arrow. Helical conformations are represented by straight lines, and random coil conformations are depicted by wavy lines.

coil swivel between S-2 and S-1, the two heads are taken to be independent.

The existence of a random coil region at the end of long S-2 is a statistical effect arising from the fewer number of conformations that can be helical at the end relative to the middle of a molecule. If, somehow, the free energy of the random coil states were raised, then the system would spontaneously undergo a coil-to-helix transition. One way of raising the free energy of random coil states is to constrain the ends and thus reduce their configurational degrees of freedom. We showed in the previous section and in Appendix A how important this effect can be within the coiled coil region itself, and how it acts to remove random coil bubbles between interacting α-helices. *(IV) Here we conjecture that in the native muscle, the attachment of S-1 to actin in a strong binding state, by restricting the allowed number of conformations of the random coil states in S-2, acts equivalently and produces a coil-to-α-helix transition at the NH_2-terminal end of S-2. The concomitant lengthening of the helical region of S-2 produces the push required to rotate S-1 and is thus the origin of the power stroke in muscle contraction.* The stability of the random coil region in the other chain depends only on whether its own head is strongly bound to actin. Thus, the model is consistent with the known independence of the two heads in the generation of tension, and is a concrete realization of some conjectures of Highsmith et al. (1979). Finally, it is consistent with experimental evidence that S-1 rotates during tension generation (Borejdo et al., 1979; Huxley, 1971; Shimizu, 1979).

NATURE OF THE S-1–ACTIN ATTACHMENT

(V) As the helix content of the force-generating region grows it causes the end of S-2 to push against S-1. For this force to produce a net rotation in S-1 and a net translation of the thin filament, the axis of rotation of S-1 must lie above the point of contact of the S-1 to the actin. If S-1 simply rolled on the surface of the actin, it would not exert any force in the direction of the muscle contraction. Proceeding by analogy, if one imagines S-1 to be an oar, and the coil-to-helix transition to provide the force due to the rower, there must be the equivalent of a thole so that S-1 does not simply rotate about its point of contact to the surface of actin, but pushes the thin filament in the direction of muscle contraction. Actually, if the surface of contact between S-1 and actin is bumpy so that they touch over a region rather than at a point, this would be sufficient to insure that the axis of rotation lies somewhere within S-1. Similarly, if there is a cavity in actin into which S-1 inserts, much like a stick into a hole, the rotation axis of S-1 will lie above the surface of the actin, and thus the rotation of S-1 could impart a force in the direction of contraction. The two mechanisms mentioned above are just some of the possible modes of attachment of S-1 to — actin that would allow the rotating S-1 to impart a force on actin in the direction of muscle contraction.

Since muscle contraction is essentially a constant volume process (Huxley, 1969; Elliot et al., 1963), the distance between the thick and thin filaments must increase during contraction. Thus, with respect to the laboratory, the rotation axis in S-1 must also move downwards towards the thin filament as S-1 rotates. Otherwise the thin and thick filaments would be pulled closer together. Finally, *nothing is known about whether the axis of rotation remains fixed or changes position within S-1 during the course of contraction. In the interest of simplicity, we assume the former situation holds* (although the latter is not a priori excluded in the formalism presented below).

While the present theory produces a concrete realization of the microscopic origin of the tensile force, namely a coil-to-helix transition, it cannot specifically address the mechanism and detailed dynamics of the S-1–actin attachment in the strong binding state. However, if the coil-to-helix mechanism is correct, it does provide some necessary conditions for the nature of the attachment.

SCHEMATIC REPRESENTATION OF THE MODEL

A schematic representation of the model is shown in Fig. 4, *A–D*. For clarity, only one of the two myosin heads is shown. As in all continuous theories of conformational transitions, the size of the random coil region is fluctuating and only average conformations are depicted. Moreover, we recognize, as first pointed out by Huxley (1957), that the fixed lattice of actin and myosin filaments responds to the overall behavior of the ensemble of crossbridges, and not to an individual crossbridge (Eisenberg and Hill, 1985). Thus, the conformations shown represent an average over the crossbridge ensemble. In all cases the coiled coil portion of S-2 is free to bend continuously as required.

In Fig. 4 *A*, S-1 is in the weak binding state (Eisenberg et al., 1968; Huxley, 1969; Huxley and Simmons, 1971), and either is completely detached from actin or remains attached for too short a time for the topological constraint to be effective in producing the coil-to-helix transition and concomitant tension generation.

Fig. 4 *B* depicts the beginning of the power stroke. In this stage, when S-1 containing ADP strongly binds to the thin filament with an angle of attachment, θ, of 90° (Reedy et al., 1965; Moore et al., 1970), the free energy of the random coil states in the force-generating region is raised because of the increased constraint. The free energy associated with the conformational transition of the swivel region from the highly random coil conformation to the highly helical conformation is available to do work. Thus, the topological constraint exerted by S-1 on the random coil in the swivel provides the mechanism of free energy transduction. The formation of the strong binding state
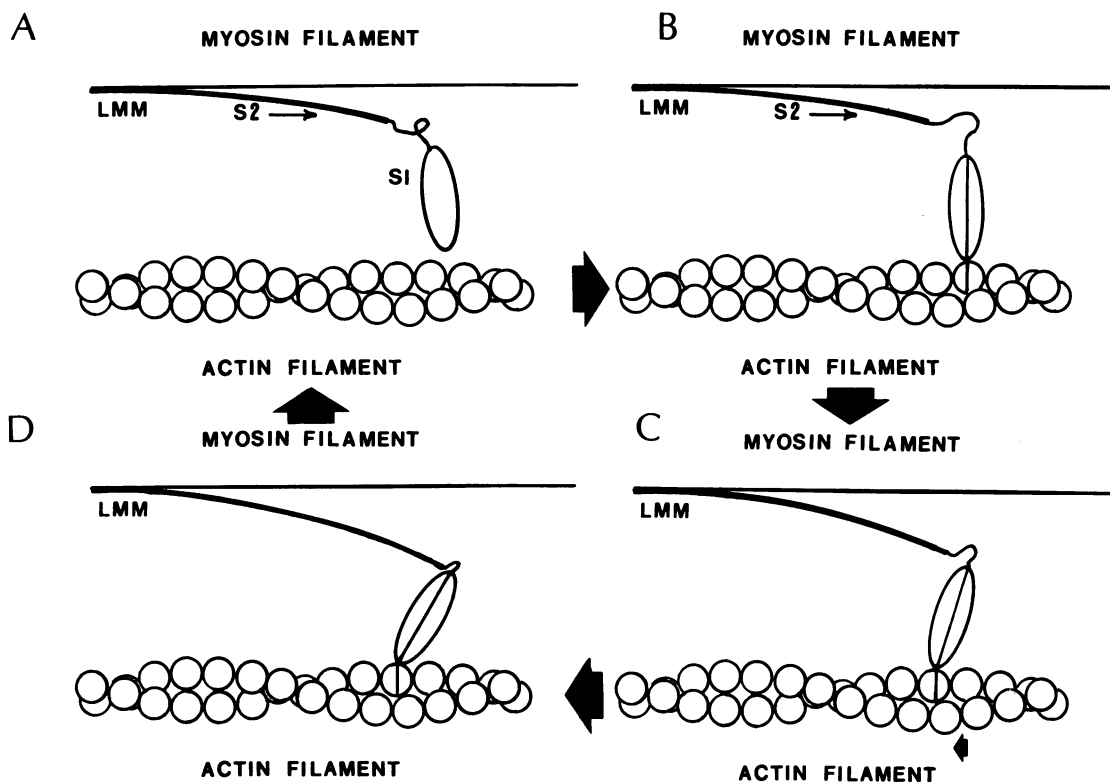
FIGURE 4 Schematic representation of the coil-to-helix transition model of tension generation. For clarity only one of the two heads of myosin is shown. (A) S-1 is in the weak binding state, and the swivel region is highly randomly coiled. (B) S-1 is in the strong binding, 90° state. The crossbridge is at the beginning of its power stroke and the force-generating region has a very low helix content. This is the conformation associated with the maximum isometric tension. (C) Partial helix formation in the swivel region with concomitant rotation of S-1 pushes the actin filament to the left as shown by the solid arrow. (D) Schematic representation of the myofilament assembly at the end of the power stroke. The force-generating region is now highly helical.

between the S-1 and actin requires that S-1 pass over an activation energy barrier. Thus, the process has a specific rate constant (Eisenberg and Hill, 1985). Fig 4 B shows the conformation associated with the maximum isometric tension, in which a force has been generated, but where there has been no net conformational change or net displacement of the thin filament.

If the fixed lattice of actin is allowed to move, the force-generating element at the end of S-2 will undergo a coil-to-helix transition, thereby causing S-1 to rotate, moving the actin along with it. Such an intermediate conformation, showing partial formation of helix in the swivel region, is shown in Fig 4 C where the direction of contraction is to the left. We assume for simplicity that
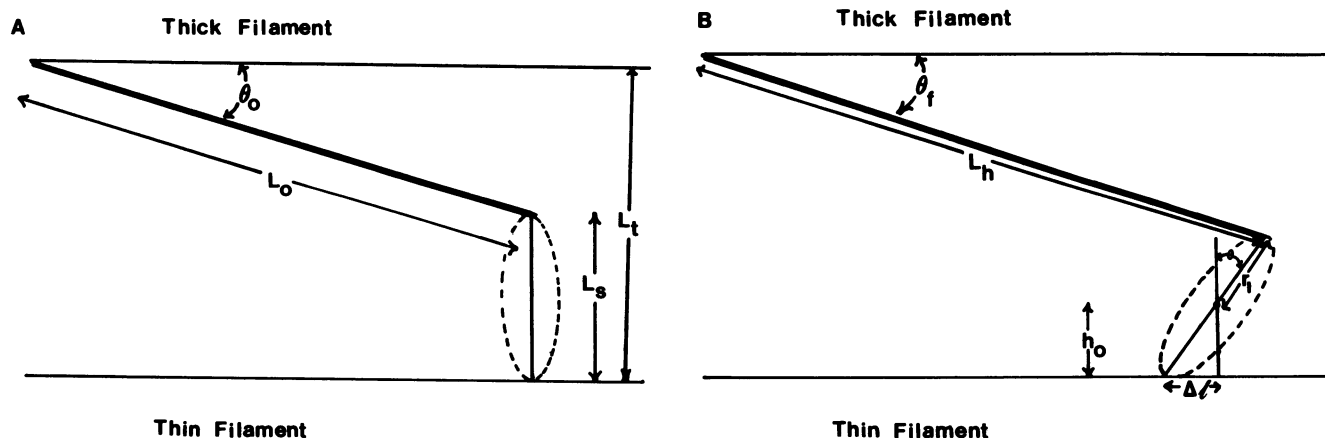

FIGURE 5 (A) Distances and angles (not to scale) associated with the strong binding 90° configuration of S-1 to actin. (B) Distances and angles (not to scale) associated with the strong binding configuration of S-1 to actin at any point during the power stroke.

S-1 when attached to the actin remains rigid and does not undergo a global conformational change. Equivalently a portion of S-1 could be rigidly bound to actin and a global conformation change within S-1 could also occur; then a piece of S-1 rotates and pushes the subfragment containing the S-1–actin complex to the left. The free energy of the force-generating region continuously decreases as the helix content increases and is available to do work. Moreover, the coil-to-helix transition is continuous and occurs gradually, which is consistent with crossbridge models of Eisenberg and Greene (1980).

Once the coil-to-helix transition has been completed, the force-generating region is now highly helical. A schematic representation of the thick–thin filament assembly at the end of the power stroke is shown in Fig. 4 D. Once the ADP is released, the S-1–actin complex remains in the strong binding state depicted in Fig. 4 D and experiences no net force (the helical regions are now at equilibrium with respect to the strong binding state). Once an additional molecule of ATP is added, the myosin returns to the weak binding state and rapidly detaches from the thin filament. As this does not involve any relative motion of thin and thick filaments, the force-generating region spontaneously undergoes the helix-to-coil transition. We make the assumption here that *(VI) a weak binding state can occur at any orientation; because the time S-1 spends in contact with actin is short, no net force is generated.* Finally, we conclude that the above mechanism is consistent with the kinetic model of Stein et al. (1979) and maintains the essential qualitative features of the Eisenberg–Green (1980) crossbridge model, with the exception that strained 90° states are not required to exist, and we decouple the orientation of S-1 from the strength of the binding state.

GEOMETRIC RELATIONSHIPS

Before proceeding to a simple mathematical realization of the coil-to-helix transition model of muscle contraction, we formulate below the various geometric relationships required in not only the present model, but also in any model of muscle contraction. As defined in Fig. 5 A, L_0 is the average distance from the attachment point of S-2 on the thick filament to the NH$_2$-terminal end of the chain of interest, when S-1 is at right angles to the thin filament. (That is, the system is at the stage depicted in Fig. 4 B.) θ_0 is the corresponding angle between L_0 and the thick filament. L_s is the linear distance from the S-1–S-2 junction point to the end of S-1. (The ellipse indicates the two-dimensional projection of the schematic shape of S-1.) Equivalently, L_s is the linear distance from the NH$_2$-terminal end of S-2 to the surface of actin when S-1 is in the strong binding, 90° conformation. L_t is the distance from the surface of the thick filament to the surface of the thin filament. *(While L_t changes continuously throughout the entire course of muscle contraction, it changes at most by ~0.3% per crossbridge cycle and is treated as a* constant for a given cycle in the calculations described below.)

Consider now the situation depicted in Fig. 5 B where S-1 is not necessarily at the beginning of the power stroke. L_h is the average linear distance in S-2 from its point of attachment to the thick filament to the NH$_2$-terminal end, and θ_f is the angle L_h makes with the thick filament. Futhermore r_1 is the linear distance from the axis of rotation of S-1 to the S-1–S-2 junction. θ is the angle between r_1 and vertical; h_0 is the distance from the axis of rotation in S-1 to the thin filament, and $\Delta\ell$ is the linear displacement of the thin filament. In what follows, the subscript max refers to the value of variables at the end of the power stroke. Thus, for example θ varies from zero (the value at the beginning of the power stroke) to θ_{max} at the end of power stroke. Experiments indicate that θ_{max} is ~45° (Moore et al., 1970; Huxley and Simmons, 1971) and that $\Delta\ell$ varies from zero to a $\Delta\ell_{max}$ of ~100 Å (Huxley and Simmons, 1971; Barden and Mason, 1978). We point out that h_0 will depend on θ and L_h, since L_t is assumed to remain constant. Elementary trigonometric analysis gives θ, h_0, θ_0, and θ_f in terms of L_s, L_t, L_0, L_h, $\Delta\ell$, and r_1. In particular, the extent of angular rotation of S-1 is given by

$$\theta = \sin^{-1}[\Delta\ell/(L_s - r_1)], \qquad (1)$$

and the distance of the axis of rotation to the thin filament is

$$h_0 = (L_s - r_1)\cos\theta. \qquad (2)$$

Thus, Eq. 2 establishes that with respect to the laboratory the axis of rotation moves down towards the thin filaments as the crossbridge rotates. Furthermore,

$$\theta_0 = \sin^{-1}[(L_t - L_s)/L_0] \qquad (3)$$

$$\theta_f = \tan^{-1}\left\{\frac{[L_0 \sin\theta_0 + L_s(1 - \cos\theta)]/L_h}{[L_0 \cos\theta_0 + r_1 \sin\theta]/L_h}\right\}. \qquad (4)$$

In Eq. 4 the quantities in the numerator and denominator are the sin θ_f and cos θ_f, respectively.

In Eqs. 1–4, two parameters, L_s and L_t, that can be estimated from structural studies enter into the calculation of the geometric quantities. $\Delta\ell$ may also be obtained from experiment (see for example, Ford et al., 1977). Additionally, *we require r_1, a quantity that is in principle dependent on $\Delta\ell$*; however, this dependence is unknown. As mentioned above, for the sake of simplicity, *we treat it as a constant.* r_1 in fact depends on the precise details of the nature of S-1–actin binding and the pathway taken by S-1 as it reorients on the surface of actin. Since the transforming part is a relatively small fraction of S-2 (the helix content of S-2 in solution at low temperatures where muscles were known to work [Ford et al., 1977] is >90% [Cohen and Szent-Györgyi, 1957; Sutoh et al., 1978; Stafford, 1985]), L_0 and L_h are likely to be close to each other, making differences in these quantities very hard to detect.

SIMPLE REALIZATION OF COIL-TO-HELIX TRANSITION MODEL OF MUSCLE CONTRACTION

In this section, we develop a simple realization of the conjectured coil-to-helix transition mechanism, with the aim of demonstrating that such a model is in qualitative and at times semiquantitative accord with a variety of experimental measurements on contracting muscle. The reader interested in the qualitative results of the theory may easily skip this section and go on to the Calculations section.

Each chain of long S-2 is taken to contain a total of $N_T = 440$ residues (Lu and Wong, 1985). *Let us divide S-2 into two regions. One region remains completely helical throughout the temperature range of interest and lies on the COOH-terminal side of S-2 and contains n_0 residues. The force-generating region at the NH_2-terminal end of S-2 is composed of n residues, which in solution have a very low helix content.* We recognize that the definitions of n_0 and n are somewhat arbitrary, and a full statistical mechanical theory that sums over all n_0, n pairs can be developed. However, for illustrative purposes we consider the simplest case here. Moreover, in the low temperature range where myosin is highly helical the more general treatment and the simple model proposed below are essentially equivalent. Since the heads occupy considerable space there must be a region at the end of the coiled coil where the chains separate from each other much like a "Y." Thus, we further assume that helical residues in the force-generating element are non-interacting with the neighboring chain. (The removal of interhelical interactions also acts to decrease the helix content of the chains in the chain separated portion of the "Y." This provides another source of the conjectured low helix content of the swivel region.)

Before the attachment of the crossbridge, the force-generating element has a very low helix content and is at equilibrium. Once attachment of a given myosin head to actin occurs, the force-generating region will spontaneously tend to undergo a coil-to helix transition. However, because it is constrained by the matrix of thin filaments (Huxley, 1957), an individual swivel region cannot undergo the conformational transition to an α-helix unless the ensemble of crossbridges moves. Thus, the myosin molecule is constrained to be in a higher free energy state and will exert a force on the thin filaments. Since the free energy of the system decreases with increasing length, then along the direction of the coil-to helix transition the change in Helmholtz free energy is

$$dA = -f dL_h. \qquad (5)$$

As the coil to helix transition progresses, $dL_h > 0$, $f > 0$ and dA decreases until $dA = 0$ in the equilibrium state. We shall assume that *the average internal energy of the ensemble of force-generating regions depends only on* *temperature and not on configuration.* Thus we need an expression for the entropy change as a function of extension of the helix; to obtain such an expression, we proceed very much in the spirit of the theory of an ideal rubber (Flory, 1953).

Consider now the ensemble of force-generating elements characterized by a progress variable α. Let $\alpha = 0$ correspond to the state where the crossbridges are attached at the beginning of the power stroke and where the force f is related to the maximum isometric tension per crossbridge (see below, Eqs. 14a and 14b). In other words at $\alpha = 0$, no displacement of the thin filament has occurred. Let $\alpha = 1$ correspond to the equilibrium distribution of conformational states in the presence of the topological constraint, i.e., the distribution of helical states at the end of the power stroke where $f = 0$.

Since the size of the force-generating element is taken to be relatively small, *we assume that the helix propagates from the coiled coil portion of the myosin rod and thus initiation of non-interacting helical stretches not contiguous to the coiled coil region of S-2 is unimportant.* (The treatment can of course be later generalized to include such states; these refinements will be incorporated into the theory subsequently.) *Finally, we treat the force-generating region as being homopolymeric with an effective helix propagation parameter s_{eff} that is the geometric mean value obtained from the amino acid sequence of the n residues in the NH_2-terminal region of S-2.*

Suppose in a given cycle there are N crossbridges in the strong binding state attached to the thin filaments. If we let P_{n_h} be the probability of a given molecule having n_h helical residues in the force-generating region and if N_{n_h} molecules actually possess n_h helical residues, we have the standard expression for the Boltzmann entropy change for the ensemble of conformations at a given α relative to that when $\alpha = 1$ (Flory, 1953). As mentioned above, the $\alpha = 1$ state is tentatively identified as the equilibrium configuration

$$\Delta S(\alpha) = S(\alpha) - S(1) = N k_B \sum_{n_h = 0}^{n} \frac{N_{n_h}}{N} \ln \left(P_{n_h} \frac{N}{N_{n_h}} \right). \qquad (6a)$$

Thus, the calculation of ΔS requires the fraction of molecules that has n_h residues in the helical state

$$p_{n_h}(\alpha) = N_{n_h}/N. \qquad (6b)$$

Now consider a fictitious system having the same overall helix content as the real system and whose random coil states are subject to the same topological constraints but whose helix propagation parameter, s_f, is smaller than that of the real system s_{eff}. (s_f must be less than s_{eff} otherwise the fictitious system will have a higher helix content.) The two systems are identical in every way except that the real system is subject to an external force that acts to maintain the helix content at the given low value and the fictitious system is not. *Thus, we make the standard assumption*

(see for example, Flory, 1953) that the relative fraction of molecules in a given state in the constrained and deformed system under stress is equal to the equilibrium value in a constrained system not under stress, but whose helical states have been destabilized relative to the state with α = 1. Thus,

$$p_{n_h}(\alpha) = s_f^{n_h} \delta_2(n_c) Z^{-1}(\alpha),$$ (6c)

with $\delta_2(n_c)$ the statistical weight of the $n_c = n - n_h$ random coil states experiencing the topological constraint due to the binding of S-1 to actin. An expression for δ_2 is derived in Appendix B, Eqs. B3 and B4. $Z(\alpha)$ is the partition function of the system and is given by

$$Z(\alpha) = \sum_{n_h=0}^{n} s_f \delta_2(n_c)$$ (6d)

and

$$s_f = s_{eff} \exp[-(1 - \alpha)g].$$ (6e)

Physically, $(1 - \alpha)g$ is the free energy in units of $k_B T$ due to the destabilization of α-helical states resulting from the external force.

Rewriting Eq.6a we find

$$\frac{\Delta S(\alpha)}{N k_B} = \sum_{n_h=0}^{n} p_{n_h}(\alpha) \ln[p_{n_h}(1)/p_{n_h}(\alpha)].$$ (7)

In Eq. 7, we recognize that P_{n_h} is given by Eq. 6c with α = 1. Thus, ΔS = 0 when α = 1, and we have correctly identified Eq. 7 with the decrease in entropy on compressing the topologically constrained force-generating element from its equilibrium extended length.

On using Eqs. 6a–c, we find

$$\Delta S(\alpha)/N k_B = \ln[Z(\alpha)/Z(1)] + (1 - \alpha)g\langle n_h \rangle$$ (8a)

with $\langle n_h \rangle$, the average number of residues that are helical, given by

$$\langle n_h \rangle = \sum_{n_h=0}^{n} p_{n_h}(\alpha) n_h.$$ (8b)

Moreover, the maximum amount of work that can be done per crossbridge

$$\Delta A(\alpha) = -T\Delta S/N,$$ (9)

with ΔS given in Eq. 9a.

Furthermore, the average length of the force-generating element is given by

$$L(\alpha) = \sum_{n_h=0}^{n} p_{n_h}(\alpha)\ell(n_h)$$ (10a)

with

$$\ell(n_h) = n_h a + b(n - n_h)^{1/2}.$$ (10b)

a is the axial translation per α-helical residue and is taken to be 1.5 Å, and b is the effective bond length divided by $\sqrt{3}$ and is taken to be 4.6 Å (Hawkins and Holtzer, 1972).

Thus, the average linear distance to the NH_2-terminal end of S-2 from the point of attachment of S-2 to the thick filament is

$$L_h(\alpha) = n_0 a + L(\alpha).$$ (11)

On setting α = 0, we obtain the expression for L_0. Actually L_h is somewhat less than that given by Eq. 11, since myosin is a continuously deforming rod; however, we use this expression in this initial, simplified version of the theory.

The force per crossbridge exerted in the direction of the coil-to-helix transformation, f, follows from

$$f = -\left(\frac{\partial \Delta A}{\partial L_h}\right)_T.$$ (12a)

But $A = A(\alpha)$ and $L = L(\alpha)$, so that

$$f = -(\partial A/\partial \alpha)_T \bigg/ \left(\frac{\partial L_h}{\partial \alpha}\right)_T.$$ (12b)

Evaluating the derivatives gives

$$f = k_B T(1 - \alpha)g[\langle n_h^2 \rangle - \langle n_h \rangle^2]/$$
$$\cdot [\langle n_h \ell(n_h) \rangle - \langle n_h \rangle \langle \ell(n_h) \rangle]$$ (12c)

where the ensemble average of a quantity, $\langle q \rangle$, is given by

$$\langle q \rangle = \sum_{n_h=0}^{n} p_{n_h}(\alpha) q(n_h).$$ (12d)

As dictated by thermodynamics, we find that when α = 1, $f = 0$ and $\Delta A(\alpha) = 0$; that is, α = 1 is the equilibrium state which minimizes the free energy.

In the limit that $g \to \infty$, i.e., for initial states of vanishing small helix content, it follows from Eq. 12c that

$$f = \frac{-k_B T}{[\ell(1) - \ell(0)]} \ln[\langle n_h \rangle (1 - 1/n)].$$ (13)

Here, $\ell(n_h)$, defined previously in Eq. 10b, is the root-mean-square end-to-end distance of the force-generating region containing n_h helical residues.

What is measured experimentally is not f, but the force along the direction of contraction, taken here to be the $-x$ direction. The magnitude of this force, f_x, is

$$f_x = f \cos \theta_f \left(\frac{\partial L_{hx}}{\partial \Delta \ell}\right)_T.$$ (14a)

Here, L_{hx} is the x component of the linear distance from the end of S-2 to the point of attachment of S-2 to the thick filament and is given by $L_h(\alpha) \cos \theta_f$ (see Fig. 5, A and B). $\Delta \ell$ is the average displacement of the actin filament in the $-x$ direction. We remind the reader that the coil-to-helix transition is in the direction opposite to the muscle contrac-

tion. S-1 acts like a lever in magnifying the distance of displacement; a small change in L_{hx} on the order of 10–20 Å is magnified into a larger change in $\Delta\ell$ on the order of 100 Å.

If we assume that the *axis of rotation is located at the point within S-1 that does not translate in the direction of contraction throughout the entire power stroke,* then elementary calculus gives

$$f_x = \frac{f r_1}{(L_s - r_1)} \cos \theta_f. \tag{14b}$$

We shall use Eq. 14b in what follows. Eq. 14b implies that if the variation in $\cos \theta_f$ is small over the entire range of interfilament spacings, then f_x should be essentially independent of the extent of thin–thick filament overlap; such independence appears to be required by experiment (Page and Huxley, 1963; Gordon et al., 1966; Huxley, 1969). We investigate whether the theory predicts that this is indeed the case below.

The one final point we need to address is the determination of g, defined in Eq. 6e. g is chosen such that when $\alpha = 0$, ΔA, the maximum amount of reversible work the system can do and given by Eq. 9, equals the total area under the reversible force, f_x, vs. $\Delta\ell$ curve. (Strictly speaking, we should equate the area under the curve to the fraction of ΔA expended in the x direction, ΔA_x; however, ΔA and ΔA_x differ by <1.5%.) In practice of course, the actual work done is always less than ΔA, but this method does provide an estimate of g, albeit crude. r_1 is then obtained by calculating f via Eq. 12c and using the experimentally determined isometric tension per crossbridge. Eq. 11 allows us to calculate L_0 and L_h. Along with the input parameters, L_s and L_t and $\Delta\ell_{max}$, we use Eq. 1 to obtain θ_{max}, and Eqs. 3 and 4 to obtain θ_0 and θ_f. Furthermore, it must be recognized that knowledge of f alone doesn't fully specify the path since the relationship of L_h to θ is unknown. To calculate f_x, a priori, also requires knowledge of r_1. Unfortunately, experimental information is not yet available for these geometric quantities. Thus, we make reasonable assumptions below and then see what the theory yields.

CALCULATIONS

In the following we set $N_T = 440$ residues (Lu and Wong, 1985); $L_s = 160$ Å (Wegener, 1982), a value for S-1 consistent with hydrodynamic measurements (although we recognize there is considerable controversy about L_s in the literature [Craig et al., 1986]); $\Delta\ell_{max} = 100$ Å (Huxley and Simmons, 1971; Barden and Mason, 1978); and $n = 24$. Studies of the theoretically calculated helix probability profiles at high helix content (Skolnick, 1983), show that $n = 24$ is a reasonable number for the penetration depth of the random coil region. Moreover, even if the force-generating region is entirely in the random coil state, the helix content of the S-2 region of myosin would be ~94.6%,

in agreement with the observed high helix content of myosin rod at low temperature (Stafford, 1985). We have also undertaken a series of studies as a function of n and find the qualitative conclusions described below remain unchanged. Finally, we set $L_t = 190$ Å (Huxley, 1969), for our initial fits; however, as discussed in further detail below the results are independent of L_t for 160 Å < $L_t \leq 230$ Å. We again remind the reader that we must specify at a given L_h, either θ or $\Delta\ell$. These depend on the properties of the S-1–actin attachment and as such are beyond the scope of the present theory.

To fit to the data, we must first relate f_x to the fractional extent of contraction, x_ℓ, defined by

$$x_\ell = \Delta\ell/\Delta\ell_{max}. \tag{15}$$

We obtained the functional form of the f_x vs. x_ℓ length profile by picking data points from Fig. 2 of Harrington's paper (1979), which is based on the experimental data of Ford et al. (1977) at 2.5°C, and we also assumed an isometric tension per crossbridge of 2.18 × 10^{-12} N. This gives,

$$f_x = \sum_{i=1}^{4} a_i (1 - x_\ell)^i, \tag{16}$$

where $a_1 = 2.0686$, $a_2 = 4.6570$, $a_3 = -6.3081$, and $a_4 = 1.7622$. The resulting f_x vs. x_ℓ curve along with the points used in the fit are shown in Fig. 6. Integration of Eq. 16 as a function of x_ℓ gives ΔA equal to 1.36 × 10^{-20} joules per crossbridge as required by the data of Ford et al. (1977).

s_{eff}, the geometric mean value of the helix propagation parameter in the force-generating region, is obtained from
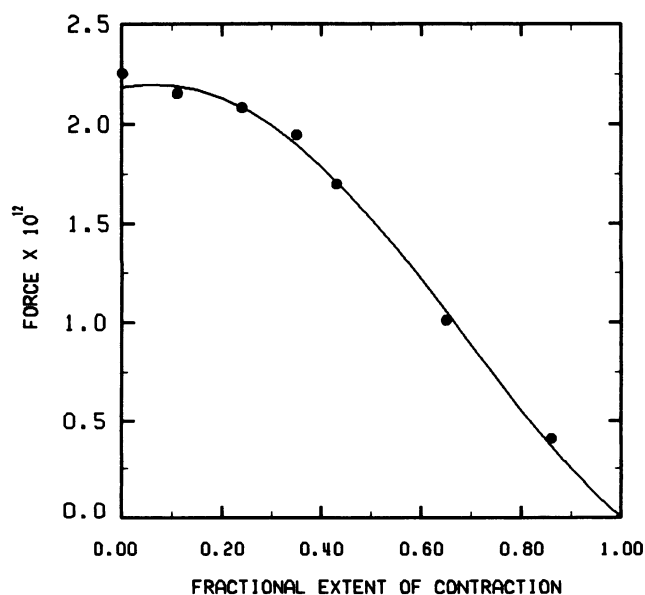

FIGURE 6 Based on the data of Ford et al. (1977), the tensile force, in newtons, generated per crossbridge vs. fractional extent of contraction per crossbridge cycle and assuming a maximum isometric tension of 2.18 × 10^{-12} N per crossbridge.

the NH_2-terminal sequence of myosin prepared from rabbit back muscle (Lu, 1980). Using the compiled table for s of Scheraga (see Skolnick and Holtzer, 1982a, b; Holtzer et al., 1983), we find that $s_{eff} = 0.974$ at 2.5°C. The results of our calculations for this system are summarized in the first row of Table I. The detailed prescription for the calculation of the various quantities is summarized at the end of the previous section.

In excellent agreement with an experimental value for θ_{max} of ~45° (Reedy et al., 1965; Moore et al., 1970; Huxley, 1969; Huxley and Simmons, 1971; Heuser and Cooke, 1983), the present theory predicts the angle of attachment of S-1 at the end of the power stroke to be 41.9°. Moreover, the present theory predicts a maximum angle between S-2 and the thick filament of ~6.2°. This is in qualitative accord with crosslinking experiments that indicate that a significant fraction of S-2 lies near the thick filament at both near neutral and alkaline pH; when under the latter conditions S-1 has moved away from the thick filament (Sutoh et al., 1978). For example, if we assume S-2 must be within 10 Å of the thick filament to crosslink, then ~33% (14%) of S-2 is close enough to the thick filament to crosslink at the beginning (end) of the power stroke.

To test the sensitivity of the results to the choice of s_{eff}, we include in row two of Table I the analogous set of calculations for $s_{eff} = 1.02$. Row three shows results for a choice of $n = 44$ and $s_{eff} = 0.974$; the insensitivity of the geometric quantities to the choice of n is evident. We should point out that a similar analysis of the data of Huxley and Simmons (1971, 1972) gives the work done per crossbridge as 1.93×10^{-20} joules per crossbridge at 4°C, which is ~50–60% of the value calculated from the actual performance of frog muscle (3.06×10^{-20} joules per crossbridge). Results for this system obtained by scaling Eq. 16 by the ratio 1.93/1.36 are shown in Table I, row four. Finally, we examine a hypothetical system having the ΔA equal to the observed work done per crossbridge in vivo in row 5 of Table I. In the latter two rows of Table I, we

also examine the sensitivity of the geometric parameters to the explicit functional form assumed for the loop entropy. We set the exponent γ in δ_2 defined in Eq. B3 equal to 1.5 rather than unity as was done for the first three cases.

Clearly, the quantity most sensitive to the details of the calculation is r_1. This reflects the strong dependence of f on the value of s_{eff}. For example, for the first two entries in Table I, when $\alpha = 0$, f changes from 31×10^{-12} to 18.2×10^{-12} N as s_{eff} goes from 0.974 to 1.02. Basically when s_{eff} decreases, the initial state helix content is lower (3.3% vs. 10.0%) and there is a greater driving force for the coil-to-helix transition to occur. On the other hand, none of the geometric parameters θ_0, θ_f, and θ_{max} are appreciably changed in all five cases studied, reflecting the insensitivity of L_0 and L_h to the details of the calculation. Since the behavior of all five systems is qualitatively similar, in the interest of brevity, we shall focus on the properties of the system described in the first row of Table I.

FREE ENERGY CHANGE vs. THE FRACTIONAL EXTENT OF CONTRACTION

In Fig. 7, we plot ΔA obtained from Eq. 9 vs. x_ϱ for the force-generating region having $n = 24$, $s_{eff} = 0.974$ at 2.5°C. As expected, since ΔA has a minimum at $x_\varrho = 1$, in this neighborhood it is a quadratic function of $(1 - x_\varrho)$; this gives rise to the linear region in the f_x vs. x_ϱ curve shown in Fig. 6. In a similar fashion, the plateau region in f_x vs. x_ϱ is a consequence of the essentially constant slope of ΔA near $x_\varrho = 0$. Neglecting the cos θ_f term, which at most introduces errors of ~0.6% into ΔA, we have from Eq. 16 that

$$\Delta A = \sum_{i=1}^{4} a_i (1 - x_\varrho)^{i+1}/(i + 1). \quad (17)$$

TABLE I*
SUMMARY OF CALCULATIONS

$n=$	s_{eff}	f_x‡	ΔA§	g	r_1‖	θ_{max}¶	θ_0¶	θ_f¶	L_0‖	L_h‖
24	0.97	2.18	1.36	0.830	10.39	41.94	2.66	6.20	647.4	660.0
24	1.02	2.18	1.36	0.430	17.12	44.42	2.65	6.54	649.0	660.5
44	0.97	2.18	1.36	0.632	15.00	43.60	2.75	6.65	625.9	656.8
24	0.97	3.11	1.93	1.00	12.21	42.58	2.66	6.29	647.3	660.6
24	1.10	4.89	3.06	1.34	14.16	43.29	2.66	6.40	647.1	660.7

*Calculated assuming $N_T = 440$, $L_t = 190$ Å, $L_s = 160$ Å, $\Delta \ell_{max} = 100$ Å, and $T = 2.5$°C in the first three rows and row five and $T = 4$°C in row four.

‡Maximum isometric tension in N per crossbridge $\times 10^{12}$.

§Work done in joules per crossbridge $\times 10^{20}$.

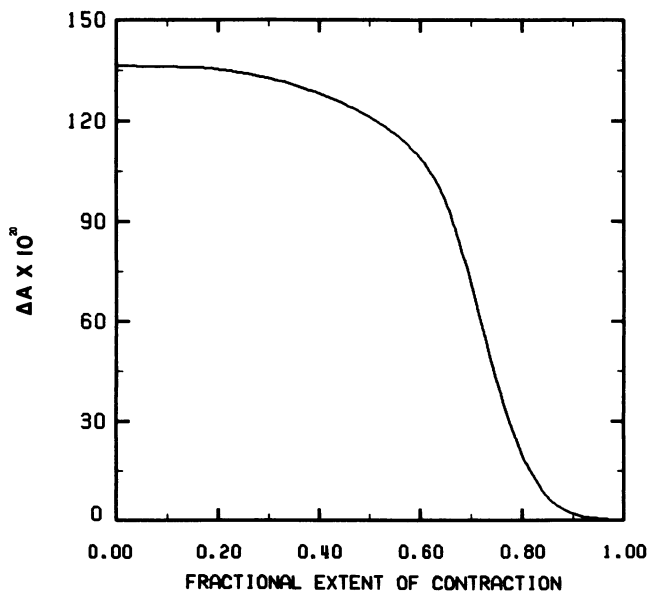‖In angstroms.

¶In degrees.

FIGURE 7 Plot of free energy in joules per crossbridge, ΔA, vs. the fractional extent of contraction, x_ϱ, for the force-generating region having $n = 24$ and $s = 0.974$ at 2.5°C.

HELIX CONTENT vs. FRACTIONAL EXTENT OF CONTRACTION

In Fig. 8, we plot the average helix content of the force-generating region, f_h obtained from Eq. 8b, vs. the fractional extent of contraction per crossbridge cycle, x_ℓ. f_h increases monotonically from the value of 3.3% at the beginning of the power stroke to ~85.6% at the end of the power stroke. Since the force-generating region is not fully helical, even at the end of the power stroke the random coil region can impart an elastic component to the tension response of muscle, in agreement with experiment (dos Remedios et al., 1972; Cooke, 1981; Naylor and Podolsky, 1981). Moreover, always being partially randomly coiled, it also acts as a swivel allowing the S-1 to rotate. While the precise values of the initial and final state helix contents depend on the choice of parameters, the qualitative behavior is the same for all cases we have examined. Moreover, we emphasize that the helix content is a highly nonlinear function of x_ℓ. (In general the relationship between the distance of S-2 from its point of attachment to the thick filament and x_ℓ is also very nonlinear; see Eqs. 2–4.) At the start of the power stroke, in the very low helix content region, the tension is very large (reflecting the system's strong desire to propagate helix at the expense of random coil), but eventually decreases as the mean helix content increases.

This simple realization of the model gives an overall helix content of S-2 at the beginning of the power stroke of 94.7% and at the end of the power stroke of 99.2%. Unfortunately such differences in helix content would be very difficult, if not impossible to measure by standard circular dichroism (CD) or optical rotary dispersion

(ORD) techniques. Direct spectroscopic probes located within the force-generating region that examine differences in mobility or average orientation attendant to the growth of helix may be required to test the validity of the present model.

Finally, we should point out that while the T_2 vs. x_ℓ curve can be simply related to the work done, the behavior of the tensile force vs. length after an abrupt length change (T_1) (Ford et al., 1977) depends in a very complicated fashion on the response of the S-1–actin complex as well as the kinetics of the coil-to-helix transition and is beyond the scope of the present simple equilibrium treatment.

DEPENDENCE OF THE FORCE ON VARIABLE FILAMENT SPACING

Physically, *(VII) it seems reasonable that the properties of the strong binding state of S-1 to actin are independent of the orientation of S-2 with respect to the thick filament* (the two regions are several hundred angstroms apart). Thus, we assume that r_1 and θ remain independent of L_t, the interfilament spacing. In Fig. 9, we plot for the system defined in the first row of Table I, θ_0 and θ_f, obtained from Eqs. 3 and 4, vs. L_t in the curves denoted by squares and circles, respectively. In the small θ_0 and θ_f limit, from Eqs. 3 and 4 it follows that θ_0 and θ_f are proportional to L_t; these linear relationships are clearly evident in the plot. Over the entire range of L_t examined, the ratio of the maximum isometric tension when $L_t = 160$ Å to that when $L_t = 230$ Å differs by <0.6% from unity. Similarly, the ratio of the force at the end of the power stroke when $L_t = 160$ Å to that when $L_t = 230$ Å differs by <1.2% from unity. Thus the present model predicts that the force generated per crossbridge is essentially independent of filament spacing,
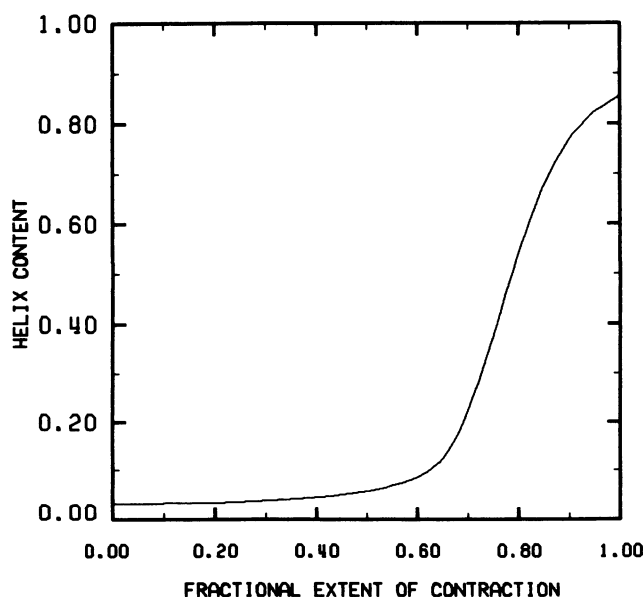
FIGURE 8 Helix content of the force-generating region vs. the fractional extent of contraction for the force-generating region having $n = 24$, $s_{eff} = 0.974$, and $T = 2.5°C$.
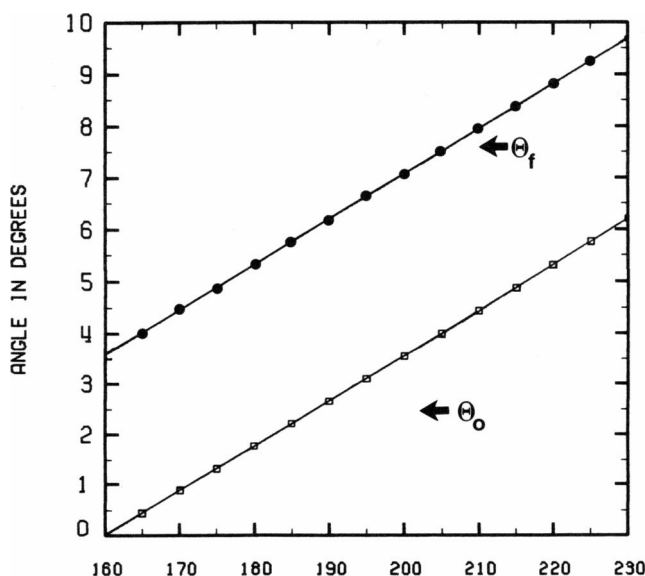
FIGURE 9 Plot of θ_0 and θ_f vs. L_t for the force-generating region having $n = 24$ and $s_{eff} = 0.974$ in the curves denoted by open squares and filled circles, respectively.

in accord with experiment (Page and Huxley, 1963; Gordon et al., 1966; Huxley, 1969).

TEMPERATURE DEPENDENCE OF THE ISOMETRIC TENSION

Measurements on frog muscle fibers indicate that the isometric tension increases by ~50% when the temperature is raised from 0.1° to 8°C (Ford et al., 1977). This is simply rationalized in the context of the present model as follows. On increasing the temperature, the helix content in the unconstrained force-generating element will decrease. Thus, after attachment of S-1 to actin the initial state of the force-generating region would also be expected to have a lower helix content, and therefore a greater entropic force that drives the system to equilibrium. In fact, as shown in Eq. 13, in the limit that $f_h \rightarrow 0$, the isometric force is predicted to be proportional to the logarithm of the helix content. In Fig. 10, we plot the maximum isometric tension as a function of the initial state helix content for systems with $r_1 = 10.39$ Å. In the limit that $f_h \rightarrow 0$, the logarithmic dependence of f_x on f_h is clearly in evidence. However, as pointed out above, since the force-generating region makes up a small fraction of S-2, the minute changes in overall helix content of S-2 with increasing temperature would be very difficult to determine experimentally. For example, if the helix content of the force-generating region decreased from 3.3 to 1.6%, the overall helix content of S-2 will have decreased from 94.73 to 94.63% (these changes in helix content are within the range predicted from the helix-coil theory), and based on Fig. 10 the isometric tension will have increased from
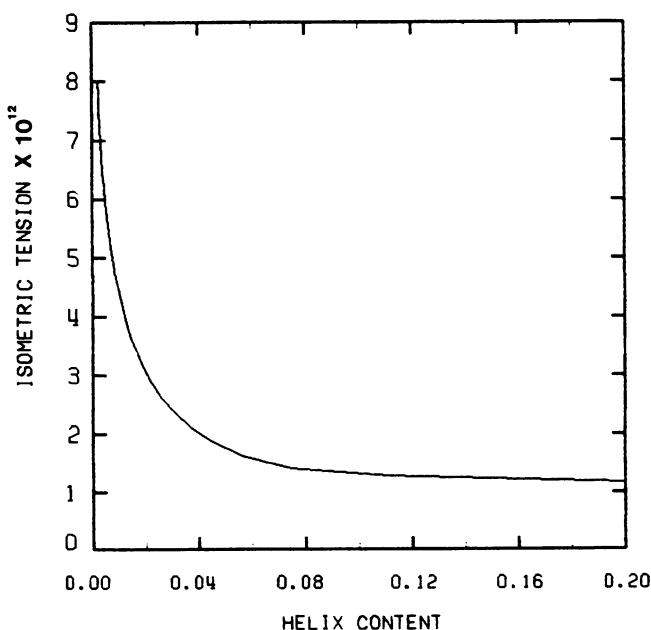

FIGURE 10   Plot of the maximum isometric tension in newtons vs. helix content for the force-generating region having $n = 24$ and assuming $r_1 = 10.39$ Å.

2.18×10^{-12} N to 3.38×10^{-12} N, an increase of 55%. Thus the large temperature dependence of the isometric tension can be rationalized.

RECAPITULATION OF THE ASSUMPTIONS OF THE COIL-TO-HELIX TRANSITION MODEL OF MUSCLE CONTRACTION

For the convenience of the reader, we collect below the assumptions used in the coil-to-helix transition model for the microscopic mechanism of muscle contraction. We first list those assumptions that form the basis of the model and subsequently list those "engineering" assumptions introduced entirely for the computational realization of the model. Justification of the various assumptions may be found above.

NECESSARY ASSUMPTIONS

(*I*) Throughout the entire course of muscle contraction, LMM remains attached to the thick filament. Long S-2 is a continuously deforming rod that allows the crossbridge to attach to actin. (*II*) In an unconstrained myosin molecule (e.g., in solution or in a weak binding state) the swivel located near the S-1–S-2 interface is due to a local random coil region in each of the chains. (*III*) Each myosin head acts independently. (*IV*) In the native muscle, the attachment of an S-1 to actin in the strong binding state, by restricting the allowed conformations of the random coil states at the NH₂-terminal end of S-2, produces a spontaneous coil-to-helix transition. The concomitant lengthening of S-2 produces the push that rotates S-1 and thus is the microscopic source of the power stroke in muscle contraction. (*V*) The nature of the S-1–actin attachment is such that the axis of rotation of S-1 lies above the thin filament, thereby allowing the rotation of S-1 attendant to the lengthening of the helical region of S-2 to impart a force to the thin filament in the direction of contraction. (*VI*) The weak binding state of the S-1–actin complex can occur at any orientation of S-1 with respect to the thin filament, but because the lifetime of the complex is short, no net force is generated. (*VII*) The properties of the strong binding state of S-1 to actin are independent of the orientation of S-2 with respect to the thin filament.

ENGINEERING ASSUMPTIONS

(*1*) Rigid S-1 attaches to the actin and pushes it along the direction of contraction. No global conformation change occurs within S-1 during the power stroke. (*2*) Within a given crossbridge cycle, the distance of separation of the thin and thick filaments is taken to be constant. (*3*) The axis of rotation of S-1 has no translational component in the direction of muscle contraction, i.e., r_1 (see Fig. 5 *B*) remains fixed. (*4*) S-2 is divided into two regions. The COOH-terminal region remains completely helical, and the NH₂-terminal region contains the force-generating region which in solution has a low helix content. (*5*) The

free energy of the coil-to-helix transition is treated by analogy to the theory of ideal rubbers. Thus, the average internal energy of the ensemble of force-generating regions depends only on temperature and not configuration, and the probability of finding a given population of molecules having n_h helical residues in the force-generating region under stress is taken to equal that of an equilibrium system whose helical states are destabilized relative to the real, unconstrained system. (6) The helix in the force-generating region of the swivel propagates from the coiled coil portion of S-2; initiation of non-interacting helical stretches not contiguous to the coiled coil region is unimportant. (7) The force-generating region is treated as a homopolymer having the same geometric mean value of the helix propagation parameter as in the real chain. (8) The denatured states of the force-generating region are treated as Gaussian random coils.

SUMMARY AND DISCUSSION

In the present paper, we have examined the possible role played by helix–coil transitions in the mechanism of muscle contraction. We conclude that because of the large free energy required to form a random coil bubble in the middle of a coiled coil, any microscopic mechanism of muscle contraction that invokes such bubbles is rather unlikely. In particular, the helix–coil transition mechanism proposed by Harrington involving the formation of a large random coil bubble is shown to require at least 25 kcal/mol of coiled coils. Even if one assumes 100% free energy transduction from ATP hydrolysis, an unlikely occurrence, and if each crossbridge acts independently as required by experiment, this still leaves ~11 kcal/mol of free energy unaccounted for. Thus, this mechanism of force generation, while not impossible, is certainly suspect unless there exists an unknown factor acting cyclically in vivo that destabilizes the coiled coil structure.

It follows from the present statistical mechanical theory that S-2 is most likely a hingeless, continuously deforming rod that swings away from the thick filament to allow for crossbridge binding at variable filament separation. We conjecture that in the absence of the strong binding of S-1 to actin, a small portion of the molecule in the swivel region between S-2 and S-1 is in the random coil state and that herein lies the force-generating region. On attachment of the myosin head to the thin filament in the strong binding state, the available conformations of the random coil in the swivel region will be reduced. The swivel region will therefore spontaneously undergo a coil-to-helix transition that causes the S-1 to rotate and pushes the thin filaments past the thick filaments. Hence, free energy transduction occurs via the topological constraints S-1 exerts on S-2 when it is in the strong binding state. The present theory is novel in that a specific, well defined spontaneous mechanism of force generation is proposed. All that is required is the attachment of the S-1 to actin, a process that is known to occur; the rest follows spontaneously.

A simple realization of the model consistent with the continuously deforming model of myosin rod and in which each myosin head operates independently predicts these features of muscle contraction, all in agreement with experiment: (a) The angle of attachment at the end of the power stroke is ~40–45°. (b) The force generated per crossbridge is essentially independent of filament spacing. (c) A significant fraction of S-2 always lies close to the thick filament. (d) Due to the tendency of the unconstrained force-generating region to have a lower helix content with increasing temperature, the isometric tension increases very steeply with increasing temperature. (e) Experimental studies on the transient response of contracting muscle to abrupt changes in length or tension indicate the presence of an elastic component. Such a component is provided in the present model by the presence of random coil regions in the force-generating element in S-2 even at the end of the power stroke where helix content is maximal. Furthermore, the theory provides a maximum free energy available to do work that is of the correct order of magnitude, without any extraneous, nonphysical assumptions, and the model is consistent with kinetic models of muscle contraction involving ATP hydrolysis.

In addition to the above, the model can predict certain quantities that so far have been unmeasurable by experiment. These include the helix content of the force-generating element as a function of the fractional extent of muscle contraction, x_ℓ, and the location of the axis of rotation in S-1. If the rotation axis is assumed to be fixed within the molecule, it is estimated to lie ~10–15 Å from the point of attachment of S-2 and S-1. The theory then provides a prediction for the relationship between the x_ℓ and the angle between S-1 and the surface of actin. Furthermore, for the present model to be valid, the S-1–actin attachment must possess certain physical characteristics in the strong binding state. It must cause the axis of rotation of S-1 to lie above the actin–myosin head interface and must somehow allow S-1 to effectively rotate with respect to the actin. This may be accomplished either as assumed here by allowing a rigid S-1 to reorient relative to the actin, or by an internal conformational change occurring within S-1 to achieve the net rotation with respect to the thin filament. Part of the force required to produce such a conformational change might be furnished by the coil-to-helix transition in S-2. Thus, attention must be paid towards elucidating the mode of the S-1–actin attachment. Finally, the model points out the highly nonlinear relationship of distances and angles inherent in this, as well any other, microscopic model of muscle contraction.

Thus, we believe the present model of muscle contraction is a plausible candidate for describing some of the microscopic events of muscle contraction. It is appealing in that it provides a simple, spontaneous mechanism of force generation. However, to verify the fundamental assumption that the force-generating step involves a coil-to-helix transition is a non-trival task, in that the overall helix

content changes in myosin rod are predicted to be very small. Perhaps spectroscopic or NMR studies may provide a means of assessing the local mobility changes within the swivel region when S-1 and actin are in the strong binding state. Proof of this is a challenge to experimentalists. Based on the apparent qualitative agreement with a wide variety of experimental facts, it seems worthwhile to extend the simple equilibrium model developed here to a more general treatment and to develop a theory for the kinetics of the coil-to-helix transition to see if characteristic experimental signatures are predicted; these are likely areas for future research.

APPENDIX A

Calculation of the Free Energy of Random Coil Bubble Formation

The statistical mechanical theory we use below treats the conformational transition in coiled coils in the spirit of single chain helix–coil theory (Zimm and Bragg, 1959), which assigns to each residue an intrachain helix initiation parameter, σ, and propagation parameter, s, and to account for interchain helix–helix interactions, the theory uses the parameter w (Skolnick and Holtzer, 1982a). Physically, $-k_B T \ln w$ is the free energy of a pair of positionally fixed and interacting α-helical turns relative to that when the α-helical turns are non-interacting. (Here k_B is the Boltzmann constant and T is the absolute temperature.) In principle, $w(T)$ depends on the specific amino acids involved and accounts for the mutual stabilization of the pair of α-helical turns due to hydrophobic interactions in the a and d positions of the quasirepeating heptet of the amino acid sequence as well as the possibility of salt bridge formation (Lu and Wong, 1985). (However, unlike the case of tropomyosin [Hodges et al., 1972; Mak et al., 1980] the amino acid sequence in the hinge region possesses a "T" spacer residue at position 62 that shifts the quasirepeating heptet [Lu and Wong, 1985].) We shall assume in the discussion presented below that w is site independent, although this is by no means required.

The free energy change in solution, ΔG_s, for the process depicted in Fig. 1 and associated with converting the fully helical myosin rod to a molecule containing a constrained random coil bubble containing m residues per chain in the hinge region of S-2 and flanked by two pairs of interacting helices is given by

$$\Delta G_s = G_{coil} - G_{helix} \tag{A1a}$$

with

$$G_{coil} = -k_B T \ln \sigma_{eff}^2 - k_B T \ln \delta(m). \tag{A1b}$$

In Eq. A1b, the first term arises from increase in free energy associated with the initiation of a second helical stretch in each of the two chains. σ_{eff} is taken to be the geometric mean value of the helix propagation

parameters in the hinge region, and from the table of Scheraga et al. (Skolnick and Holtzer, 1982; Holtzer et al., 1983), we find that $\sigma_{eff} = 3 \times 10^{-4}$. $-k_B T \ln \delta(m)$ is the loop entropic term and represents the reduction in configurational entropy when the two ends of a random coil containing $2m$ residues are constrained to form a closed loop relative to the case where the ends are free. Assuming the chain is Gaussian, we can use the well known result that

$$\delta(m) = C_1/(2m)^{3/2}. \tag{A1c}$$

Previously we have estimated $C_1 = 0.23$ (Skolnick, 1985b), although it may in fact be smaller. Moreover, the exponent of $\delta(m)$ for a real chain with excluded volume lies closer to 2.0 (de Gennes, 1979); thus Eq. A1c is a conservative estimate for $\delta(m)$.

Furthermore,

$$G_{helix} = -k_B T \ln s_{eff}^{2m} - k_B T \ln w^{m/3.5}. \tag{A1d}$$

In Eq. A1d, G_{helix} is the free energy of the $2m$ fully helical residues in the hinge region of S-2 containing $m/3.5$ interacting pairs of α-helical turns when it is flanked by two pairs of interacting helical stretches. s_{eff} is the geometric mean value of the helix propagation parameter in the hinge region of S-2. Using the table of Scheraga et al. (Skolnick and Holtzer, 1982; Holtzer et al., 1983), we find $s_{eff}(T) = 0.931$ at 37°C. Finally, at 37°C we estimate that $w = 1.97$, a value obtained by fitting the thermal denaturation profile based on myosin rod (Stafford, 1985) of a hypothetical homopolymeric analogue (Holtzer, A., and J. Skolnick, unpublished results). (By way of comparison this is substantially less than the value of w in tropomyosin which equals 2.34 at 37°C [Skolnick and Holtzer, 1985].)

Using Harrington's estimate that $m = 201$ in Eq. A1a we find that at 37°C, $\Delta G_s = +22.7$ kcal/mol of molecules containing random coil bubbles, of which loop entropy contributes +6.4 kcal/mol to the free energy destabilization. Actually, Harrington's original estimate of the size of the force-generating element is in error. In his calculation, he uses the mean square end-to-end distance of a random coil, $\langle R^2 \rangle$, in the calculation of the size of the force-generating element. Actually, since the shortening is along the direction of contraction, what is required is the mean-square end-to-end distance along a particular direction. Thus, he should have used $\langle R^2 \rangle/3$, which then gives $n = 146$ and $\Delta G_s = +20.7$ kcal/mol of coiled coils to which loop entropy contributes $\sim +6.2$ kcal/mol.

For a myosin molecule attached to both the thin and thick filaments in vivo, we have to correct Eq. A1b for the fact that the two interacting helical regions experience a reduction in the allowed relative angular orientation of the two helices. Assuming that the orientation of the myosin attached to the thick filament remains unchanged when the force-generating element undergoes the helix–coil transition, the free energy change in vivo

$$\Delta G_{mus} = \Delta G_s - k_B T \ln (\delta\Omega/4\pi). \tag{A2}$$

The quantity $-k_B T \ln \delta\Omega/4\pi$ accounts for the reduction in orientational freedom of the second pair of α-helices relative to the case where they are free to adopt any angular orientation. $\delta\Omega$ is the solid angle accessible to the second helical region at the NH$_2$-termini of S-2, consistent with the attachment of S-1 to the actin filament. If the NH$_2$-terminal helices lie within 10° of their parallel orientation to the thick filament (a reasonable value, see Table I) and are capable of moving over an angle $\phi = 27.8°$ that allows the head to move a distance of 54.6 Å (approximately equal to the diameter of the actin helix [Huxley, 1969] which is certainly a gross overestimate), then $-k_B T \ln \Omega \approx +4.6$ kcal/mol. Thus, even if we use the conservative estimate that $\Delta G_s = +20.7$ kcal/mol, we find that it requires in vivo $\sim +25.3$ kcal/mol of coiled coils to cause formation of the constrained random coil bubble containing 146 residues per chain.

APPENDIX B

Statistical Weights of Constrained Random Coil States in the Force-generating Region of S-2

On attachment of the S-1 to actin, the end-to-end vector in the random coil portion of S-2, r, is constrained to effectively lie in one dimension. The origin of this is as follows. The NH$_2$-terminal end of S-2 follows a curvilinear path $L_0 + \ell$ as function of θ (or equivalently α). While r can move along the coordinate defining the direction of the coil-to-helix transition, ℓ, it is constrained by its attachment to S-1 to lie in the other two dimensions within a small element of area dA. Moreover, negative values of the end-to-end vector are physically impossible given the constraint that S-1 is attached to actin; i.e., only r and $\ell \geq 0$ are allowed. Thus, the statistical weight of the n_c random coiled residues in the force-generating element is given by

$$\delta_2(n_c) = \left(\frac{3}{2\pi}\right)^{3/2} (n_c b_0^2)^{-3/2} \, dA \int_0^\infty d\ell \exp\left\{-\frac{3}{2}\ell^2/n_c b_0^2\right\} \quad (B1)$$

$$\delta_2(n_c) = \frac{3}{4\pi} \, dA (n_c b_0^2)^{-1}. \quad (B2)$$

Assuming $dA = (dV)^{2/3}$, with $dV = 359 \text{ Å}^3$ (Skolnick and Holtzer, 1985) we have if $n_c > 0$

$$\delta_2(n_c) = 0.19/(n_c)^\gamma \quad (B3)$$

with $\gamma = 1$, and if $n_c = 0$

$$\delta_2(n_c = 0) = 1. \quad (B4)$$

REFERENCES

Barden, J., and P. Mason. 1978. Muscle crossbridge stroke and activity revealed by optical diffraction. *Science (Wash. DC)*. 199:1212–1213.

Bernengo, J. C., and R. Cardinaud. 1982. State of myosin in solution. Electric birefringence and dynamic light scattering studies. *J. Mol. Biol.* 159:501–517.

Borejdo, J., S. Putnam, and M. F. Morales. 1979. Fluctuations in polarized fluorescence: evidence that muscle cross-bridges rotate repetitively during muscle contraction. *Proc. Natl. Acad. Sci. USA*. 76:6346–6350.

Cardinaud, R., and J. C. Bernengo. 1985. Electric birefringence study of rabbit skeletal myosin subfragments HMM, LMM and rod in solution. *Biophys. J.* 48:751–763.

Chen, C. L., and J. Skolnick. 1986. Theory of the helix-coil transition in singly crosslinked, two-chain, coiled coils. 2. Role of mismatched states. *Macromolecules*. 19:242–243.

Cohen, C., and A. G. Szent-Györgyi. 1957. Optical rotation and helical polypeptide chain conformation and α-proteins. *J. Am. Chem. Soc.* 79:248–250.

Cooke, R., and K. E. Franks. 1978. Generation of force by single headed myosin. *J. Mol. Biol.* 120:361–373.

Cook, R. 1981. Stress does not alter the conformation of a domain of the myosin crossbridge in rigor muscle fibers. *Nature (Lond.)*. 294:570–571.

Craig, R., J. Trinick, and P. Knight. 1986. Discrepancies in length of myosin head. *Nature (Lond.)*. 320:688.

de Gennes, P. 1979. Scaling Concepts in Polymer Physics. Cornell University Press, Ithaca, New York. 40–43.

dos Remedios, G. G., R. G. C. Millikan, and M. F. Morales. 1972. Polarization of tryptophan fluorescence from single striated muscle fibers. *J. Gen. Physiol.* 59:103–120.

Eads, T. M., and L. Mandelkern. 1984. Backbone and side chain motion in myosin subfragment 1 and rod determined by natural abundance carbon-13 NMR. *J. Biol. Chem.* 259:10689–10694.

Eisenberg, E., and L. E. Green. 1980. The relation of muscle biochemistry to muscle physiology. *Annu. Rev. Physiol.* 42:293–309.

Eisenberg, E., C. R. Zobel, and C. Moos. 1968. Subfragment of myosin. Adenosinetriphosphatase activation by actin. *Biochemistry*. 7:3186–3194.

Eisenberg, E., and T. L. Hill. 1985. Muscle contraction and free energy transduction in biological systems. *Science (Wash. DC)*. 227:999–1006.

Elliot, A., and G. Offer. 1978. Shape and flexibility of the myosin molecule. *J. Mol. Biol.* 123:505–519.

Elliot, G. F., J. Lowy, and C. R. Worthington. 1963. An x-ray and light diffraction study of the filament lattice of striated muscle in the living state and in rigor. *J. Mol. Biol.* 6:295–305.

Flory, P. J. 1953. Principles of Polymer Chemistry. Cornell University Press, Ithaca, New York. 432–475.

Flory, P. J. 1956a. Role of crystallization in polymers and proteins. *Science (Wash. DC)*. 124:53–60.

Flory, P. J. 1956b. Theory of elastic mechanisms in fibrous proteins. *J. Am. Chem. Soc.* 78:5222–5238.

Ford, L. E., A. F. Huxley, and R. M. Simmons. 1977. Tension responses to sudden length change in stimulated frog muscle fibres near slack length. *J. Physiol. (Lond.)* 269:441–515.

Goody, R. S., and K. C. Holmes. 1983. Crossbridges and the mechanism of muscle contraction. *Biochim. Biophys. Acta*. 726:13–39.

Gordon, A. M., A. F. Huxley, and F. J. Julian. 1966. The variation in isometric tension with sarcomere length in vertebrate muscle fibers. *J. Physiol. (Lond.)*. 184:170–192.

Harrington, W. F. 1971. A mechanochemical mechanism for muscle contraction. *Proc. Natl. Acad. Sci. USA*. 68:685–689.

Harrington, W. F. 1979. On the origin of the contractile force in skeletal muscle. *Proc. Natl. Acad. Sci. USA*. 76:5066–5070.

Harvey, S. C., and H. C. Cheung. 1983. Myosin flexibility. *In* Cell and Muscle Motility. Vol. 2. R. M. Dowben and J. W. Shay, editors. Plenum Publishing Corp., New York. 279–302.

Hawkins, R. B., and A. Holtzer. 1972. Some macromolecular properties of poly(α-L-glutamic acid). *Macromolecules*. 5:294–301.

Heuser, J. E., and R. Cooke. 1983. Actin-myosin interactions visualized by the quick freeze, deep etch replica technique. *J. Mol. Biol.* 169:97–122.

Highsmith, S., K. M. Kretzschmar, C. T. Okonski, and M. F. Morales. 1977. Flexibility of myosin rod, light meromyosin and myosin subfragment-2 in solution. *Proc. Natl. Acad. Sci. USA*. 74:4986–4990.

Highsmith, S., K. Akasaka, M. Konrad, R. Goody, K. Holmes, N. W. Jardetzky, and O. Jardetzky. 1979. Internal motions in myosin. *Biochemistry*. 18:4238–4244.

Highsmith, S., and R. Cooke. 1983. Evidence for actomyosin conformational changes involved in tension generation. *In* Cell and Muscle Motility. Vol. 4. R. M. Dowben and J. W. Shay, editors. Plenum Publishing Corp., New York. 207–237.

Highsmith, S., and D. Eden. 1986. Myosin subfragment 1 has tertiary structural domains. *Biochemistry*. 25:2237–2242.

Hill, T. L. 1952. Some statistical mechanical models of elastic polyelectrolyes and proteins. *J. Chem. Phys.* 20:1259–1273.

Hill, T. L. 1953. Energetics and molecular mechanisms of muscle action. II. Statistical thermodynamical treatment of contractile systems. *Faraday Soc. Disc.* 13:132–145.

Hill, T. L. 1977. Free Energy Transduction in Biology. Academic Press, Inc., New York. 116–117.

Hodges, R., J. Sodek, L. Smillie, and L. Jurasek. 1972. Tropomyosin: amino acid sequence and coiled coil structure. *Cold Spring Harbor Symp. Quant. Biol.* 37:299–310.

Holtzer, M. E., A. Holtzer, and J. Skolnick. 1983. α-Helix-to-random coil transitions of two-chain, coiled coils. Theory and experiments for thermal denaturation of α-tropomyosin. *Macromolecules*. 16:173–180.

Huxley, A. F. 1957. Muscle structure and theories of contraction. *Prog. Biophys. Chem.* 7:255–318.

Huxley, A. F. 1974. Muscular contraction. *J. Physiol. (Lond.).* 243:1–44.

Huxley, A. F., and R. M. Simmons. 1971. Proposed mechanism of force generation in striated muscle. *Nature (Lond.).* 133:533–539.

Huxley, A. F., and R. M. Simmons. 1972. Molecular transients and the origin of muscular force. *Cold Spring Harbor Symp. Quant. Biol.* 37:669–680.

Huxley, H. E. 1957. The double array of filaments in cross-striated muscle. *J. Biophys. Biochem. Cytol.* 3:631–648.

Huxley, H. E. 1969. The mechanism of muscular contraction. *Science (Wash. DC).* 164:1356–1365.

Huxley, H. E. 1971. The structural basis of muscular contraction. *Proc. R. Soc. London Ser. B Biol. Sci.* 198:131–149.

Huxley, H. E., R. M. Simmons, A. R. Faruqi, M. Kress, J. Bordas, and M. H. Koch. 1981. Millisecond time resolved changes in x-ray reflections from contracting muscle during rapid mechanical transients. *Proc. Natl. Acad. Sci. USA.* 78:2297–2302.

Hvidt, S., F. H. M. Nestler, M. L. Greaser, and J. D. Ferry. 1982. Flexibility of myosin rod determined from dilute solution viscoelastic measurements. *Biochemistry.* 21:4064–4073.

Hvidt, S., J. D. Ferry, D. Roelke, and M. Greaser. 1983. Flexibility of light meromyosin and other coiled coil α-helical proteins. *Macromolecules.* 16:740–745.

Hvidt, S., T. Chang, and H. Yu. 1984. Rigidity of myosin and myosin rod by electric birefringence. *Biopolymers.* 23:1283–1294.

Iwazumi, T. 1979. A new field theory of muscle contraction. *In* Crossbridge Mechanism in Muscle Contraction. H. Sugi and G. H. Pollack, editors. University Park Press, Baltimore. 611.

Jacobson, M., and W. H. Stockmayer. 1950. Intramolecular reaction in polycondensations. I. Theory of linear systems. *J. Chem. Phys.* 18:1600–1606.

Karn, J., S. Brenner, and L. Barnett. 1983. Protein structural domains in the Caenorhabditis Elegans Unc-54 myosin heavy chain gene are not separated by introns. *Proc. Natl. Acad. Sci. USA.* 80:4253–4257.

Kobayashi, S., and T. Totsuka. 1975. Electric birefringence of myosin subfragments. *Biochim. Biophys. Acta.* 376:375–385.

Lin, S., Y. Konishi, M. E. Denton, and H. A. Scheraga. 1984. Influence of an extrinsic crosslink on the folding pathway of ribonuclease A. Conformational and thermodynamic analysis of crosslinked (Lys[7]-Lys[41]) ribonuclease A. *Biochemistry.* 23:5504–5512.

Lu, R. C., and A. Wong. 1985. The amino acid sequence and stability predictions of the hinge region in myosin subfragment-2. *J. Biol. Chem.* 260:3456–3461.

Lu, R. C. 1980. Identification of a region susceptible to proteolysis in myosin subfragment-2. *Proc. Natl. Acad. Sci. USA.* 77:2010–2013.

Mak, A., L. Smillie, and G. Stewart. 1980. A comparison of the amino acid sequence of rabbit skeletal muscle α- and β-tropomyosins. *J. Biol. Chem.* 255:3647–3655.

Morawetz, H. 1965. Macromolecules in Solution. Interscience Publishers, New York. 121.

Mendelson, R. A., M. F. Morales, and J. Botts. 1973. Segmental flexibility of the S-1 moiety of myosin. *Biochemistry.* 12:2250–2255.

Moore, P. B., H. E. Huxley, and D. J. De Rosier. 1970. Three dimensional reconstruction of F-actin. Thin filaments and decorated thin filaments. *J. Mol. Biol.* 50:279–295.

Naylor, G. R. S., and R. J. Podolsky. 1981. X-ray diffraction study of strained muscle fibers in rigor. *Proc. Natl. Acad. Sci. USA.* 78:5559–5563.

Page, S., and H. E. Huxley. 1963. Filament lengths in striated muscle. *J. Cell Biol.* 19:369–390.

Poland, D., and H. A. Scheraga. 1969. Theory of Helix-Coil Transitions in Biopolymers. Academic Press, Inc., New York. 178–250.

Reedy, M. K., K. C. Holmes, and R. T. Tregear. 1965. Induced changes in orientation of the crossbridges of glycerinated insect flight muscle. *Nature (Lond.).* 207:1276–1280.

Rosser, R. W., F. H. M. Nestler, J. L. Schrag, J. D. Ferry, and M. Greaser. 1978. Infinite dilution viscoelastic properties of myosin. *Macromolecules.* 11:1239–1242.

Schellman, J. A. 1955. The stability of hydrogen-bonded peptide structures in aqueous solution. *Compt. Rend. Trav. Lab Carlsberg (Ser. Chim.).* 29:230–259.

Shimizu, H., M. Yano, K. Nishiyama, K. Kometani, S. Chaen, and T. Yamada. 1979. Active potential and dynamic cooperativity in the chemo mechanical conversion in active streaming and muscle contraction. *In* Crossbridge Mechanism in Muscle Contraction. H. Sugi and G. H. Pollack, editors. University Park Press, Baltimore. 563.

Skolnick, J., and A. Holtzer. 1982a. Theory of helix-coil transitions of α-helical two-chain, coiled coils. *Macromolecules.* 15:303–314.

Skolnick, J., and A. Holtzer. 1982b. Theory of α-helix to random coil transitions of two-chain, coiled coils. Application to a synthetic analog of tropomyosin. *Macromolecules.* 15:812–821.

Skolnick, J., and A. Holtzer. 1985. Theory of α-helix-to-random coil transition of two-chain, coiled coils. Application of the augmented theory to thermal denaturation of α-tropomyosin. *Macromolecules.* 18:1549–1559.

Skolnick, J., and A. Holtzer. 1986. α-Helix-to-random coil transition of two-chain, coiled coils. A theoretical model for the "pretransition" in cysteine 190-crosslinked tropomyosin. *Biochemistry.* 25:6192–6202.

Skolnick, J. 1983. Effect of loop entropy on the helix-coil transition of α-helical, two-chain, coiled coils. *Macromolecules.* 16:1069–1083.

Skolnick, J. 1984. Effect of loop entropy on the helix-coil transition of α-helical, two-chain, coiled coils. 3. Supermatrix formulation of the imperfect matching model. *Macromolecules.* 17:645–658.

Skolnick, J. 1985a. Role of topological constraints in the all-or-none transition of a globular protein model: theory of the helix-coil transition in doubly crosslinked, two-chain, coiled coils. *Biochem. Biophys. Res. Commun.* 129:848–853.

Skolnick, J. 1985b. Theory of the helix-coil transition in singly crosslinked, two-chain, coiled coils. *Macromolecules.* 18:1535–1549.

Skolnick, J. 1986. Theory of the helix-coil transition in doubly crosslinked, two-chain, coiled coils. A globular protein model. *Macromolecules.* 19:1153–1166.

Stafford, W. F. 1985. Effect of various anions on the stability of the coiled coil of skeletal muscle myosin. *Biochemistry.* 24:3314–3321.

Stein, L. A., R. Schwarz, P. B. Chock, and E. Eisenberg. 1979. Mechanism of actomyosin adenosine triphosphatase. Evidence that adenosine 5'triphosphate hydrolysis can occur without dissociation of the actomyosin complex. *Biochemistry.* 18:3895–3909.

Sutoh, K., K. Sutoh, T. Karr, and W. F. Harrington. 1978. Isolation and physicochemical properties of a high molecular weight subfragment-2 of myosin. *J. Mol. Biol.* 126:1–22.

Sutoh, K., Y. C. C. Chiao, and W. F. Harrington. 1978. Effect of pH on the cross bridge arrangement in synthetic myosin filaments. *Biochemistry.* 17:1234–1239.

Takahashi, K. 1978. Topography of the myosin molecule as visualized by an improved negative staining method. *J. Biochem.* 13:905–908.

Thomas, D. D. 1978. Large scale rotational motions of proteins detected by electron paramagnetic resonance and fluorescence. *Biophys. J.* 24:439–462.

Tsong, T. Y., T. Karr, and W. F. Harrington. 1979. Rapid helix-coil transitions in the S-2 region of myosin. *Proc. Natl. Acad. Sci. USA.* 76:1109–1113.

Wegener, W. A. 1982. A swivel jointed formalism for segmentally flexible macromolecules and its application to the rotational behavior of myosin. *Biopolymers.* 21:1049–1080.

Wilkie, D. R. 1975. Muscle as a thermodynamic machine. *Ciba. Found. Symp.* 31:327–335.

Woledge, R., N. A. Curtin, and E. Homsher. 1985. Energetic Aspects of Muscle Contraction. Academic Press, London. 24–25.

Zimm, B. H., and J. K. Bragg. 1959. Theory of the phase transition between the helix and random coil in polypeptide chains. *J. Chem. Phys.* 31:526–535.